JMEPEG
https://doi.org/10.1007/s11665-025-12397-7

1059-9495/$19.00

ORIGINAL RESEARCH ARTICLE

Study of Forming Accuracy and Surface Finish in Multi-Stage Robot-Assisted Incremental Sheet Hydroforming of AA6061

Ravi Prakash Singh, Santosh Kumar, Sudarshan Choudhary, Edward James Brambley, Pankaj Kumar Singh, and Amrut Mulay

Submitted: 28 January 2025 / Revised: 23 July 2025 / Accepted: 31 July 2025

This study presents the development of multi-stage robot-assisted incremental sheet hydroforming (MSRAISHF), an innovative process that integrates multi-stage incremental sheet forming (MSISF) with hydroforming to enhance formability, thickness uniformity, and surface finish in aluminum alloy AA6061 sheets. MSRAISHF was compared with single-stage RAISHF, revealing that multi-stage processing produced fixed wall angle conical frustums (FWACF) with improved forming depths and enhanced thickness uniformity along the wall of the cone. Notably, MSRAISHF reduced spring back by 60%, significantly improving the geometric accuracy of the formed parts. Surface quality also improved markedly, with reduced surface roughness and the suppression of undesired waviness commonly observed in single-stage RAISHF. To further assess the effect of multiple forming stages on surface characteristics, a Variable Wall Angle Stepped Conical Frustum (VWASCF) was designed. This sample was used to analyze the influence of forming stages on thickness distribution and surface finish. The results indicate that MSRAISHF is effective for producing sheet metal parts with improved surface finish and dimensional stability, making it suitable for applications requiring high accuracy and surface quality.

Ravi Prakash Singh, WMG, University of Warwick, Coventry CV4 7AL, UK; Mathematics Institute, University of Warwick, Coventry CV4 7AL, UK; and Department of Mechanical Engineering, Indian Institute of Technology, Varanasi 221005, India; **Santosh Kumar**, Department of Mechanical Engineering, Indian Institute of Technology, Varanasi 221005, India; **Sudarshan Choudhary** and **Amrut Mulay**, Department of Mechanical Engineering, SVNIT, Surat 395007, India; **Edward James Brambley**, WMG, University of Warwick, Coventry CV4 7AL, UK; and Mathematics Institute, University of Warwick, Coventry CV4 7AL, UK; and **Pankaj Kumar Singh**, Department of Mechanical Engineering, Poornima University, Jaipur 303905, India. Contact e-mail: ravi.p.singh@warwick.ac.uk.

Published online: 23 October 2025

Graphical Abstract

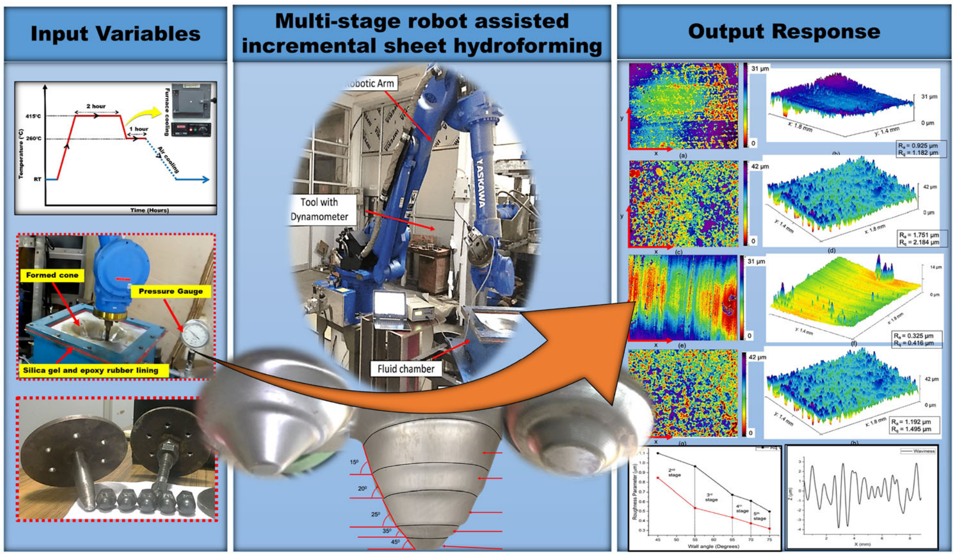

Keywords hydroforming, incremental sheet forming, spring back, straight groove test, surface finish

1. Introduction and Literature Survey

In the ever-evolving landscape of manufacturing, incremental sheet forming (ISF) has emerged as a promising alternative to conventional sheet metal forming processes especially in the realm of customized low batch production. The conventional forming methods, such as stamping and deep drawing, have long been the cornerstones of sheet metal forming, but they come with limitations in terms of tooling costs, need for dedicated dies and geometrical constraints. ISF, on the other hand, offers a paradigm shift by enabling the fabrication of complex geometries with reduced tooling requirements and enhanced process flexibility (Ref 1–5). In ISF, the deformation of sheet metal workpiece takes place through the controlled motion of tool over the surface of the sheet. Unlike traditional methods that rely on fixed dies and punches, ISF employs a localized deformation approach, where material is formed incrementally in a layer-by-layer fashion. This allows for the fabrication of intricate and customized geometries without the need for dedicated dies, thus lowering production costs and setup times. ISF has been used to produce a variety of parts for a variety of industries including aerospace (Ref 6, 7), automotive (Ref 8–10), and medical (Ref 11, 12).

In the initial years of ISF, the process was carried out using a 5/6 axis NC/ CNC machine. However, in the recent times 5/6-axis industrial robots are being used as driver machines in ISF, the process known as robot-assisted ISF (RAISF) or simply Roboforming (Ref 13). Robotic arms in ISF introduce a new dimension of flexibility, precision, and adaptability to the manufacturing landscape. They have ability to execute intricate tool paths with a high level of accuracy (Ref 14, 15). ISF is usually conducted using a single tool that maintains point contact with the sheet surface, a process commonly known as Single Point Incremental Forming (SPIF). As the other side of the sheet is free, this leads to geometrical inaccuracies, nonuniform stress distribution and large spring back in the formed component (Ref 16). To overcome these issues, ISF with flexible medium from back of sheet has been reported by researchers. The flexible medium underneath sheet act like a die and supports forming leading to improved formability, uniform strain distribution and accuracy of the formed product. In recent studies, various flexible mediums like pressurized air (Ref 17), metallic foam (Ref 18), rubber (Ref 19), and static fluid (Ref 20) have been employed from the back of the sheet in ISF to enhance formability and reduce springback. Kumar and Kumar (Ref 21) applied hydraulic fluid in ISF, and termed the process as incremental sheet hydroforming (ISHF). Khalifa and Thiery (Ref 22) applied gas as a supplementary forming tool under controlled pressure to achieve concave-convex shapes. - Shang et al. (Ref 23, 24) validated the benefits of hydraulic support in ISF through FEA modeling and experiments, finding improved thickness uniformity and maximum achievable wall angles. similarly, Küçüktürk and Yazgın (Ref 25), reported better thickness uniformity and formability in ISF under static fluid pressure.

In the recent years, researchers have also used multi-stage ISF (MSISF) globally, which involves fabricating a part across several stages leading to improved formability. Steeper wall angles can be formed using strategy of MSISF as reported by various researchers (Ref 26–28). MSISF are often used for fabricating sheets of Titanium (Ref 29, 30), steel (Ref 31, 32),and aluminum (Ref 33–35) with steeper Walls. Some researchers have investigated formability, thickness distribution and geometrical accuracy of parts formed by MSISF process. Shamsari et al. (Ref 36) examined the formability of a two-stage SPIF for maximum forming depth. It is observed that two-stage forming enhances forming depth up to 26% as compared to SPIF. Ndip- Agbor et al. (Ref 37) formed a 75° cone in seven stages with the combination of outside-in (OI) and inside-out (IO) tool path. Liu et al. (Ref 35) through FEA and experiments found that more uniform thickness distribution can be obtained in the formed part. Strength and formability of sheet metal part were reported to increase with increase in number of stages. Similar results were obtained by Verbert et al. (Ref 38) and Malhotra et al. (Ref 39) who investigated thickness distribution of parts and concluded that this process gives a more uniform thickness distribution. Dai et al. (Ref 40)studied the effect of feed rate, spindle speed and step depth on geometric accuracy of parts formed by MSISF and concluded that step depth is the most influencing process parameter. In the shape fabricated by MSISF, step marks remain at the end of the product due to accumulation of plastic strain. Nirala et al. (Ref 41) used FEA to study this unwanted feature and proposed the strategy to reduce and eliminate it. Some researchers have tried to use multi-stage incremental sheet hydroforming to take the benefits of both multi-stage ISF and ISHF. Kumar and Kumar (Ref 28) deployed multi-stage ISHF to fabricate near vertical conical frustums with wall angles up to 90°. Thiery and Ben Khalifa (Ref 42) explored multi-stage ISF with active medium, reporting that a preform height of 75% of the final product significantly reduced undesired bending due to lower vertical forces (Ref 42).

It can be understood from above literature survey that both MSISF and incremental sheet hydroforming can improve the process capabilities of ISF. Despite numerous studies on surface roughness, springback, and formability in context of ISF, very few studies have been carried out on multi-stage ISHF. The novelty of the present work lies in the integration of multi-stage tool path strategy with robot-assisted incremental sheet hydroforming (MSRAISHF), which has not been extensively explored in existing literature. MSRAISHF has been deployed to fabricate AA6061 blank. The formability, thickness distribution and surface finish of the formed product achieved in MSRAISHF has been compared with that in single-stage RAISHF(SSRAISHF). Further this study also introduces a novel geometry named variable wall angle stepped conical frustum (VWASCF) to systematically evaluate the effect of the number of forming stages on both surface finish and geometric accuracy to examine the effect of number of stages on various forming parameters such as forming angle, surface finish and thickness distribution on the formed product. A VWASCF has been fabricated using MSRAISHF and effect of number of stages on surface finish and waviness on formed product has been examined.

2. Base Material

In present study, aluminum alloy 6061 blank with a thickness of 1.05 mm was chosen due to its wide range application in sheet metal industry. To relieve the residual stress in the as received sheet and to get uniform microstructure, a solution heat treatment was administered at 415 °C for 2 h. Following this, they were cooled within a furnace to 260 °C and maintained at this temperature for an additional hour before being air-cooled (Ref 43). The heat treatment cycle followed for preparing the preform is outlined in Fig. 1.

The composition of AA6061 was determined using an optical emission spectrometer and is outlined in detail in Table 1.

To assess the material properties of the sheet before forming, uniaxial tensile test and Erichsen ductility test have been conducted. ASTM/E8 standard has been followed in preparation of samples for the tensile test (Ref 44). The mechanical properties obtained from tensile tests are given in Table 1. Further, to assess the ductility of the preform, Erichsen ductility test (Ref 45) was conducted the details of which are also presented in Table 1.

3. Experimental Setup

The experimental configuration for Robot-Assisted Incremental Sheet Hydroforming (RAISHF) has been entirely developed and patented by IIT, Varanasi, as illustrated in Fig. 2 (Ref 46). Detailed descriptions of the setup can be found in previous studies by the authors (Ref 20, 47).

Main components of the setup include a six-axis industrial robotic arm with a payload capacity of 180 kN, a controller, and a teach pendant (provided by M/s Yaskawa), along with a clamping system, forming tool, tool dynamometer for force

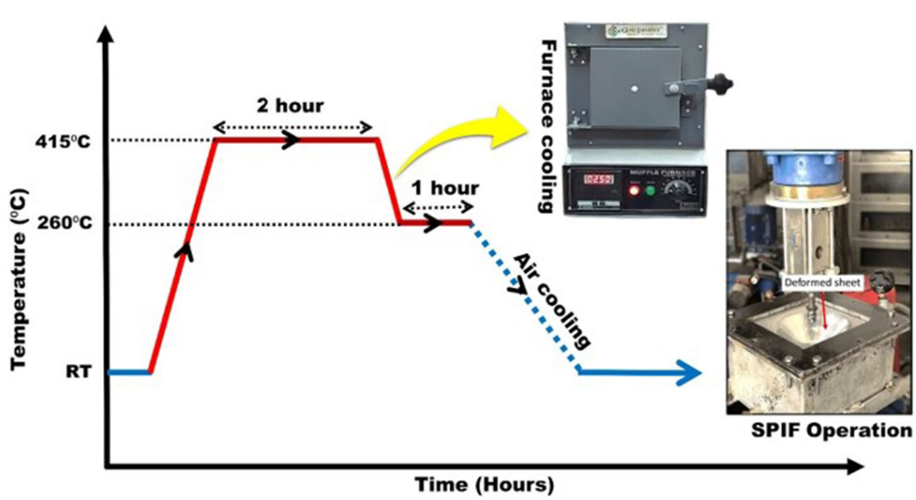

Fig. 1 Heat treatment cycle adopted for making the preform of AA6061 (Ref 43)

Table 1 Composition and Mechanical Properties of AA6061 Aluminum Alloy

Composition (wt.%)									
Elements	**Al**	**Ti**	**Si**	**Mg**	**Fe**	**Mn**	**Zn**	**Cr**	**Cu**
wt.%	97.41	0.03	0.54	0.82	0.41	0.02	0.06	0.15	0.35
Mechanical Properties									
Tensile Properties			**Erichsen Ductility (Dome Height H_D)**						
Property	**Value**		**Dome 1**	**Dome 2**	**Dome 3**				
Yield Strength (MPa)	112 ± 5		IE (mm)	9.34	9.12	8.92	Average		
UTS (MPa)	127 ± 5		H_D (mm)	9.02	8.82	8.61	$H_D = 9.13$		
Elongation (%)	12.16 ± 0.1								

measurement, a fluid chamber RAISHF, a piston-cylinder assembly for maintaining hydraulic pressure, control valves (V_1, V_2, V_3), and pressure sensors for monitoring pressure. Various parts of the setup are shown in Fig. 2(b), (c), and (d). To prevent air and fluid leakage from the fluid chamber, silica gel and epoxy rubber have been applied between the flange and the chamber. The working methodology of RAISHF is illustrated in Fig. 3(a). The fluid chamber is filled with oil before forming. The sheet is clamped between flanges and sealed using silica gel and epoxy rubber to ensure it is leak-proof and airtight. Valves V_1 and V_2 are closed, and V_3 remains open. Hydraulic pressure is applied from the back of the sheet using the piston-cylinder assembly with a counterweight. It was observed that pressures greater than 1.3 bar caused the sheet to bulge upwards, and subsequent downward tool movement resulted in folds and cracks, as shown in Fig. 3(b). Hence, an optimal pressure range between 1.0 bar and 1.3 bar has been selected. This pressure, maintained by the piston-cylinder arrangement, is not sufficient to cause any significant plastic deformation but provides support from the back of the sheet, improving geometrical accuracy and ensuring uniform strain distribution during forming. Similar recommendations have been made by Shang et al. (Ref 23, 24).

Figure 3(b) and 3(c) shows the cone formed and the corresponding pressure during the cone formation, respectively. Once forming was completed, Valve V_1 was opened to return the fluid to the reservoir.

The strategy for tool path planning adopted for SSRAISHF is shown Fig. 4(a), whereas the strategy for process of MSRAISHF is shown in Fig. 4(b).

As shown in Fig. 4(b) that for multi-stage RAISHF, the initially 45° wall angle cone is fabricated using strategy explained for single-stage RAISF. In the subsequent stages, the wall angle is increased by a certain amount $(5^\circ - 10^\circ)$ after every stage.

The experimental parameters of tool speed, tool diameter, and step depth were chosen based on the straight groove test because of its simplicity and quick execution. The groove depth, spring back, and forming time were analyzed using regression analysis to identify the best combination of input parameters. This was done using the central composite response surface design (CCRSD) in Minitab software. Tool speed and step depth were treated as continuous variables, while tool diameter was considered categorical. A total of 39 experiments were conducted, optimizing the results to minimize forming time and spring back while maximizing the theoretical depth. The optimal values were determined as: tool speed of 85 mm/s, step size of 0.4 mm, and tool diameter of 12.5 mm, achieving a composite desirability of 0.7652. These optimal parameters balanced the trade-offs between the output responses and were selected for further experimentation (Ref 48).

4. Results and Discussion

Once the setup had been developed and parameters were finalized, a variable wall angle conical frustum as suggested by Hussain et al. (Ref 49) was fabricated to evaluate the limiting forming angle which was found to be 64°. A fixed wall angle conical frustum (FWACF) of wall angle 64° was fabricated using single and multi-stage RAISHF using the strategy explained in Fig. 3 and was used for comparison.

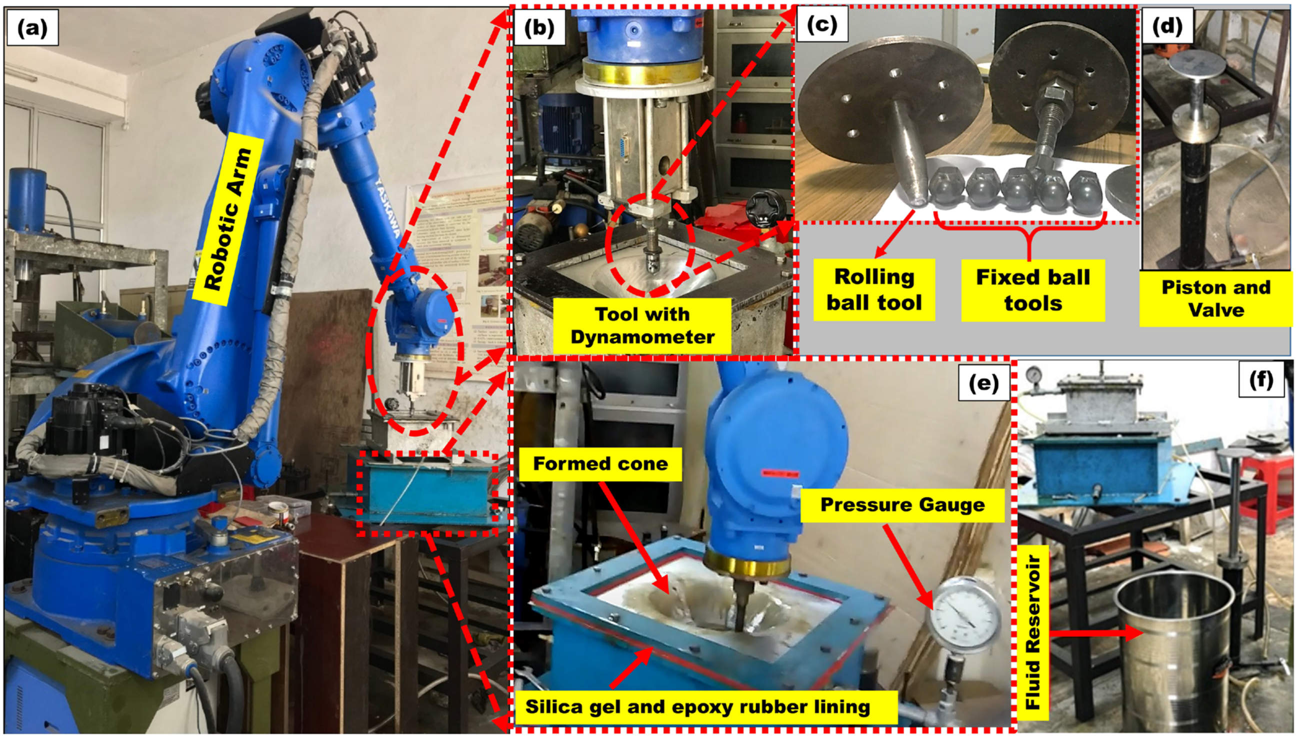

Fig. 2 RAISHF setup: (a) developed setup at IIT(BHU), (b) forming tool with tool dynamometer (c) different tools fabricated (d) piston and valve arrangement (e) fabricated cone with leak-proof fluid chamber (f) fluid reservoir

4.1 Comparison of Single and Multi-Stage RAISHF

The experimental details of the conical frustum of fixed wall angle of 64° fabricated by single and multi-stage RAISHF are given in Table 2.

It is shown in Table 2 that more forming depth can be achieved for similar wall angle of 64°. This can be directly attributed to the increased accuracy of the formed FWACF MSRAISHF in comparison to SSRAISHF. Further, it can also be seen that stepped marks are found to be left at the end of the FWACF formed by multi-stage RAISHF. Compensation forming strategies or post forming strategies could be adopted to remove these stepped marks (Ref 41).

4.2 Thickness Distribution and Accuracy Comparison

The thickness distribution of the sample made by single and multi-stage RAISHF has been examined. For this purpose, the cone has been cut meridionally using wire electric discharge machine and the length of the cone is divided in three regions which are shown in Fig. 5 (b) and (c), respectively.

The regions of the FWACF along the length of the cone are given as:

Region 1: The region of upper undeformed blank and the region of deformation of initial contours of the wall. This region undergoes combined bending and stretching.

Region 2: The middle region of the wall, where the sine law for thickness prediction is most accurate.

Region 3: The region of the lower undeformed region containing last contours of the wall.

The plot of thickness distribution along the length of the FWACF of wall angle 64° formed by single and multi-stage RAISHF is shown in Fig. 5(a). It may be observed from Fig. 5(a) that for SSRAISHF, excessive thinning happens in region 1. In region 2, the thickness was found to be uniform and can be approximated by sine law. Thickness again increases in region 3 due to the presence of an undeformed sheet near the bottom region of FWACF. Similar trends were obtained and reported by Jeswiet et al. (Ref 4) and Ambrogio et al. (Ref 50) in their work. The minimum thickness is found in region 1 due to bending and stretching taking place in this region in the initial stage of forming. In region 2, the sheet thickness is found to be uniform due to the shear mode of forming found in this zone as suggested by Jeswiet et al. (Ref 51), Kim et al. (Ref 4), Avitzur and Yang (Ref 52). In multi-stage forming, the trend is almost similar; however, the sheet is found to be slightly thinner. The thickness values for both the cases are given in Table 3.

It may be observed from Table 3 that slightly more thinning is observed in case of multi-stage RAISHF; however, more uniform strain distribution is observed in case of multi-stage RAISHF. Further, because of lack of support in the ISF process can result in unintended global deformations in addition to the intended local ones. These unintended deformations, which are challenging to manage, leads to spring back and decrease the accuracy of the final part. The spring back observed in case of FWACF can be be estimated by expressing it in terms of theoretical wall angle (θ_t) and actual wall angle (θ_a) as evaluated by expression 1

$$\theta_t = \frac{TD}{(R_0 - R_f)} \quad \text{(Eq 1)}$$

The actual wall angle (θ_a) attained in after fabrication of FWACF is less than (θ_t) due the presence of elasticity in the sheet. After the tool leaves the local contact with the sheet, there is an elastic release of deformation due to which spring

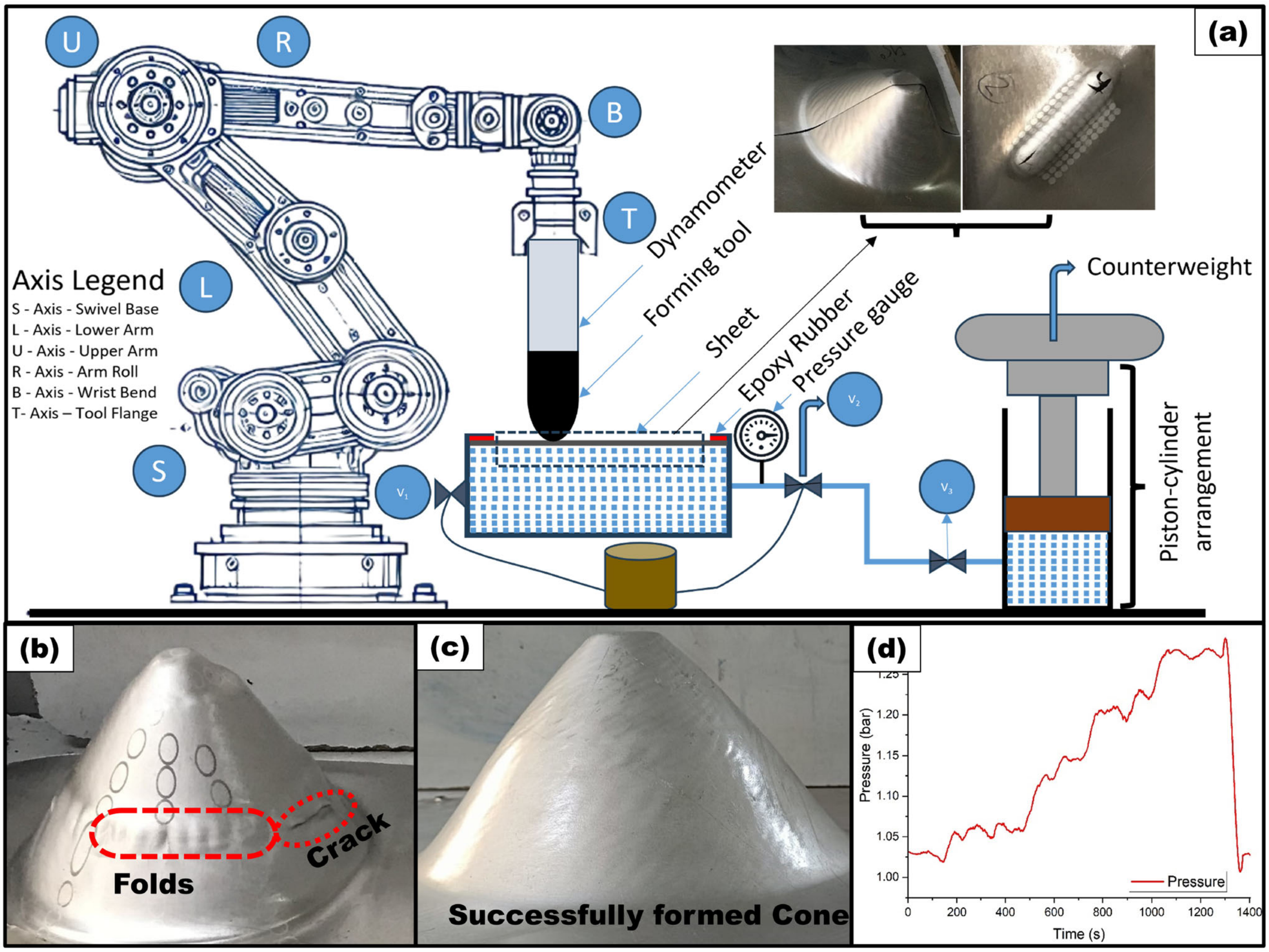

Fig. 3 (a) Schematic diagram for working of RAISHF (b) crack and fold in the sample when formed with a high back pressure (c) successfully formed cone and (d) pressure from back during successful formation of cone

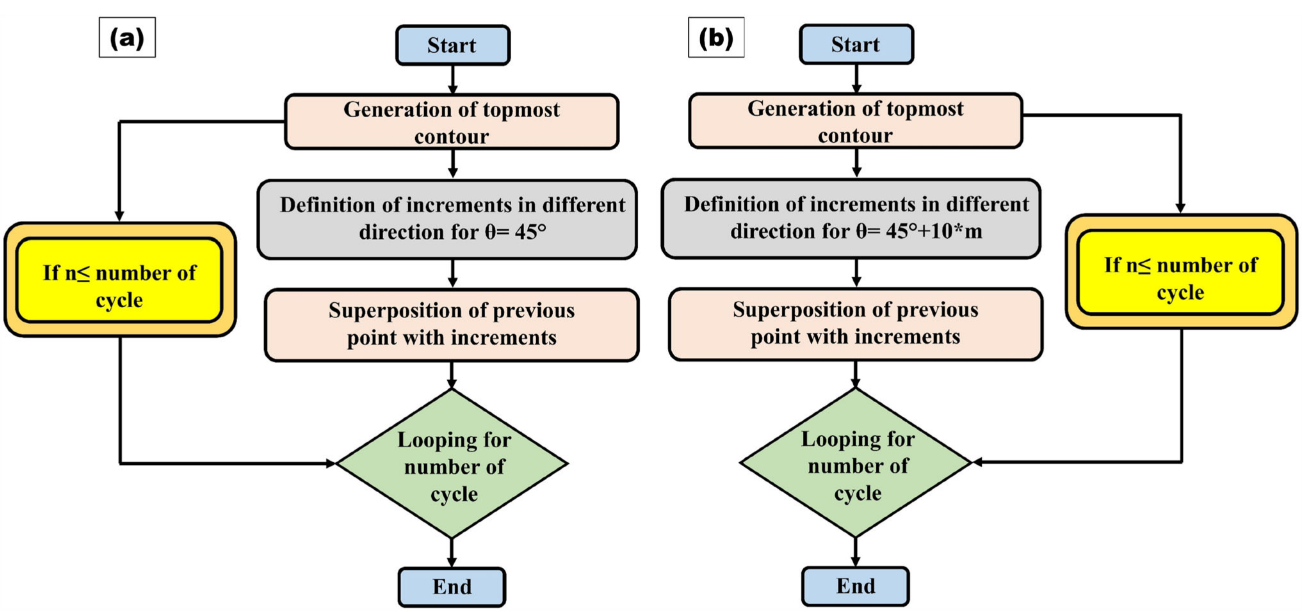

Fig. 4 Strategy for fabrication in (a) SSRAISHF (b) MSRAISHF

Table 2 Details of FWACF by single and multi-stage RAISHF

Single-stage RAISHF		Multi-stage RAISHF		
		Stage 1	Stage 2	Stage 3
Tool Diameter (mm)	12.5	12.5	12.5	12.5
Step Size (Δr)	0.2	0.4	0.275	0.2
Step Size (ΔZ)	0.4	0.4	0.4	0.4
Theoretical wall angle (°)	64	45	55	64
No of cycles run	160	160	160	160
Theoretical Depth (mm)	64	64	64	64
Actual Depth (mm)	58.32	55.57	59.41	62.56
Initial Radius (mm)	120	120	120	120
Final radius (mm)	88.02	58.13	74.09	88.01
Actual Wall angle (°)	61.26	41.92	52.30	62.91
Elastic Spring back (%)	4.27	6.82	4.90	1.69

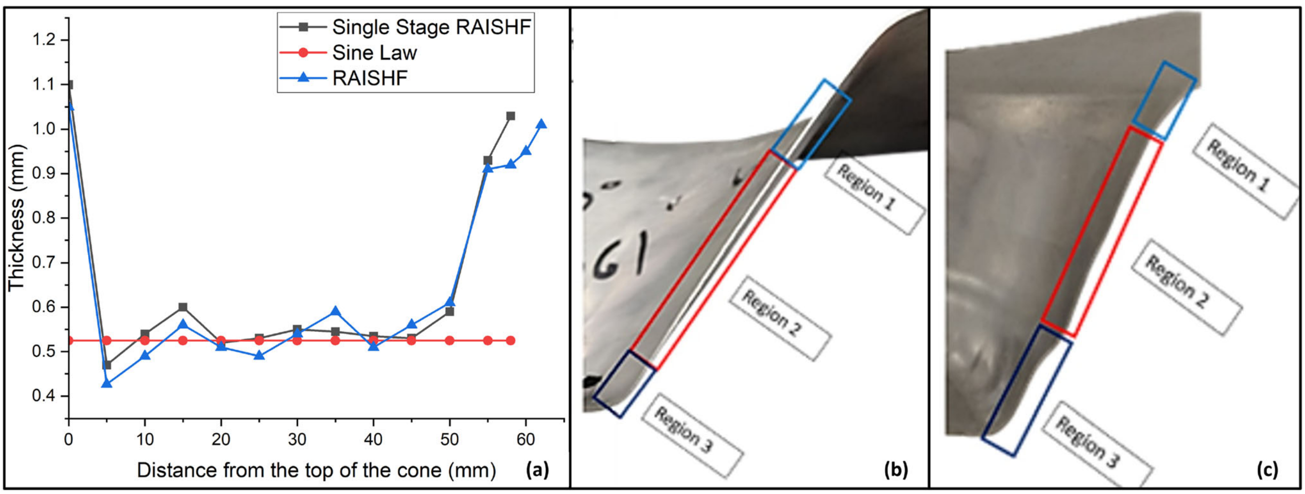

Fig. 5 (a) Thickness distribution along the length of FWACF (b) cut section of FWACF fabricated by SSRAISHF (c) cut section of FWACF fabricated by MSRAISHF

Table 3 Thickness values in single and multi-stage RAISHF

Forming method	Minimum thickness (mm)	Average thickness(mm) (Region 2)
Single-stage RAISHF	0.472 ± 0.001	0.548 ± 0.001
multi-stage RAISHF	0.431 ± 0.001	0.521 ± 0.001

back occurs. Amount of spring back occurring in the process can be evaluated by Eq 2.

$$\text{Spring back}(\%) = \frac{(\phi_t - \phi_a)}{\phi_t} \times 100 \quad \text{(Eq 2)}$$

The Spring back observed in the fixed wall angle conical frustum formed by multi-stage RAISHF was observed to be 1. 7% where as in case single-stage RAISHF spring back was found to be 4.3%.Hence, a reduction of 60.45% in spring back was observed in case of multi-stage RAISHF. Each forming stage induces additional plastic deformation in the sheet due to which forming depth increased in every stage as shown in Table 2, progressively work-hardening the material and making it less susceptible to elastic recovery. Further, sequentially deforming the sheet after each stage, ensures a balanced strain distribution across the part, which limits differential strain recovery and thus reduces spring back. Hence, it can be concluded that multi-stage RAISHF apart from being helpful in getting steeper wall angle, additionally can be responsible for more uniform strain distribution with reduced spring back and parts with ultra-high accuracy can be fabricated by using MSRAISHF strategy.

4.3 Comparison of Surface Finish in Single-Stage and Multi RAISHF

The surface quality of the formed product is a crucial parameter for determining the quality of the formed product. As there is a localized contact in ISF, the nature of contact with the sheet can deteriorate the surface quality of the formed product (Ref 53–55). To compare the surface quality of the FWACF fabricated by single and multi-stage RAISHF, their respective surface qualities have been examined. For this purpose, three samples have been taken: (a) Undeformed sample (UD), (b) Sample taken from region 2 of cone formed by single-Stage RAISHF (SS), (c) Sample taken from region 2 of cone formed by single-Stage RAISHF (MS). The surface topography and surface roughness (in terms of R_a & R_q) of these samples have been examined for surface characterization of the formed product. R_a, or arithmetical mean roughness, represents the average vertical deviation of the surface profile from its central mean line over a specified length. It gives a general sense of how smooth or rough a surface is. R_q, or root mean square roughness, is a more sensitive parameter that calculates the square root of the average of the squared deviations from the mean line, placing greater emphasis on peaks and valleys. A lower R_a or R_q value indicates a smoother surface, which is often desirable in sheet metal applications.

For surface topography, scanning probe microscope ($_S$PM) has been used. Surface roughness of the samples has been measured by R_a and R_q values, which is captured by moving the stylus knob over the sample. This test has been carried out on the MitutoyA2100 ma $R_a$ine. $_T$he sample length was 2.4 mm, the number of samples was 5. The 2D and 3D view of UD sample is presented in Fig. 6(a) and (b), respectively.

Surface characterization of both, inner and outer surfaces of the samples formed by single and multi-stage RAISHF has been also carried out. The 2D and 3D topographical micrographs of both surfaces of samples are displayed in Fig. 7(a), (b), (c), (d), (e), (f), and (g). It can be observed from Fig. 7 that tool-sheet contact in RAISHF can affect the surface quality of the formed product. The surface quality of the inner surface, which is in direct contact with the tool, gets deteriorated as FWACF is formed.

It can be seen from the 3D surface topograph and the observed R_a and R_q values of the inner surface shown in Fig. 7(b) that the surface quality is deteriorated as compared to that of the undeformed sample which naturally happens because of contact with tool and sheet. However, the surface quality of inner surface improved significantly on performing multi-stage RAISHF. It was observed that the surface finish in the cone formed after single stage had waviness present in its walls. The subsequent forming stages were applied to the preformed cones from earlier stages, effectively reducing the valleys in the wavy patterns. This approach was highly beneficial in enhancing the surface finish by smoothing out irregularities of the earlier stages and achieving a more uniform surface profile. The surface had significantly reduced nonuniformities, as seen in Fig. 7(c). In terms of R_a value also, the surface roughness was significantly improved after performing MSRAISHF. The R_a value in case of MSRAISHF reduced to $0.325\mu m$ from $0.925\mu m$ in SSRAISHF; thus, there is a significant improvement of 64.86% in surface quality of the formed product. An improvement in the surface quality of the outer surface is also observed in multi-stage RAISHF, with R_a value decreasing from 1.751 μm to 1.192 μm. It can be said that performing RAISHF in multiple stages is helpful in achieving better surface quality product which was also confirmed by measuring the surface waviness of the three samples. It was observed that the surface formed after SSRAISHF had high waviness, which is due to the state of stress which evolved due to combined bending and stretching occurring during the forming operation (Ref 3, 56). However, the surface waviness was visually found to decrease significantly after performing subsequent stages of forming. The surface waviness was characterized by measuring the valley height of the wavy patterns observed on the surface, which is given in Fig. 8. It is observed from Fig. 8 that waviness in the surface formed by MSRAISHF has significantly reduced as compared to that formed by SSRAISHF. The valley height of inner surface of FWACF formed by multi-stage RAISHF varied between $-0.73\mu m$ to $0.26\mu m$, whereas that formed by SSRAISHF, it varied from $3.07\mu m$ to $1.46\mu m$. The outer surface of the cone formed by both the processes has more surface irregularities in form of waviness than the inner surface. However, out of the two outer surfaces, the cone formed by MSRAISHF has less waviness as can be seen from Fig. 8(b) and (d). Thus, it may be concluded that performing MSRAISHF can improve surface quality significantly. It does not only ensure less surface roughness than SSRAISHF, but waviness is also significantly reduced which a major problem in ISF.

4.4 Effect of no of Forming Stages in RAISHF

For assessing the effect of number of forming stages, A varying wall angle stepped conical frustum (VWASCF) has been fabricated. Starting with wall angle of 45°, the wall angle was increased by 10° in first two stages and by 5° for the subsequent stages as explained in Fig. 4(b). The experimental details of VWASCF fabricated by RAISHF are given in Table 4 and the detailed diagram of VWASCF is presented in Fig. 9. VWASCF has been fabricated to examine the effect of number of stages in MSRAISHF. As shown in Fig. 9, the topmost section has undergone maximum no of forming stages (N). The section right below the immediate top section has undergone (N-1) forming stages and so on. Once the samples had been fabricated, they were tested for thickness distribution and surface finish which are discussed in upcoming sections.

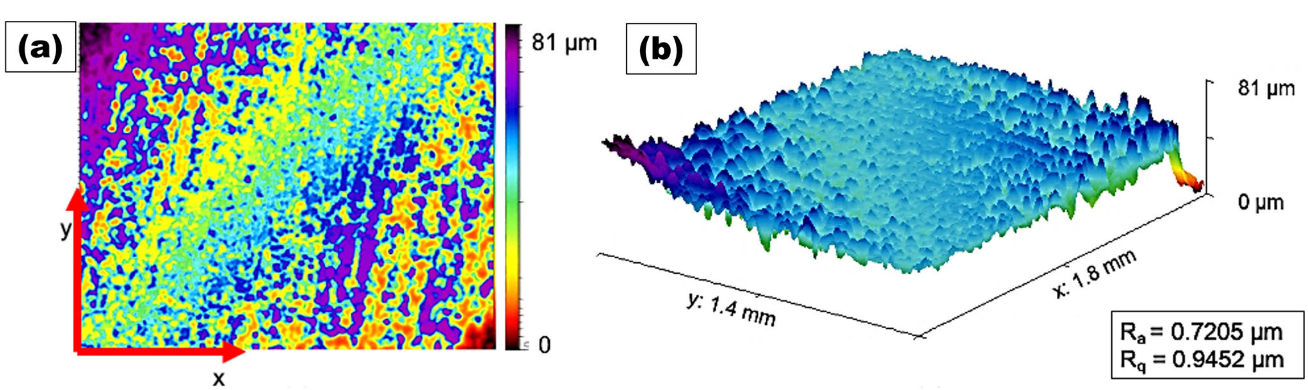

Fig. 6 Topographic micrograph of undeformed sample in (a) 2D and (b) 3D

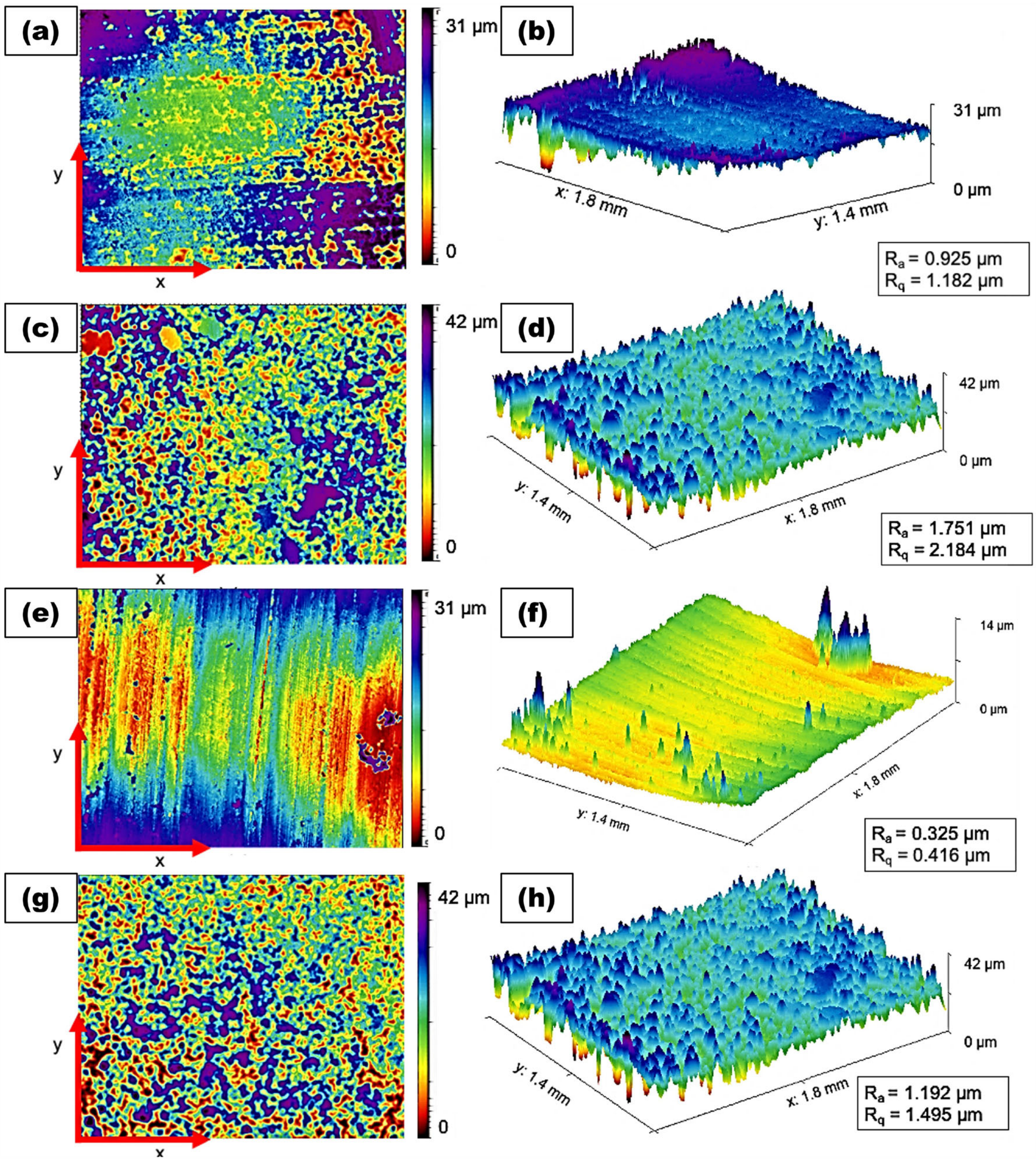

Fig. 7 2D and 3D micrographs of different surfaces: (a) 2D topographical micrograph of inner surface of single stage (SS), (b) 3D topographical micrograph of inner surface of SS, (c) 2D topographical micrograph of outer surface of SS, (d) 3D topographical micrograph of outer surface of SS, (e) 2D topographical micrograph of inner surface of multi-stage (MS), (f) 3D topographical micrograph of inner surface of MS, (g) 2D topographical micrograph of outer surface of MS, (h) 3D topographical micrograph of outer surface of MS

4.4.1 Thickness Distribution and Spring Back in VWASCF. VWASCF was cut meridionally, and the thickness at various locations was measured as mentioned earlier. The value of sheet thickness along the length of VWASCF is shown in Fig. 10. It is observed from Fig. 10 that in the top region of the cone, the sheet underwent maximum thinning, and hence the thickness in this region is minimum. This is because this region of VWASCF underwent maximum stages of forming making its wall angle to be maximum. As the depth of cone increases, the wall angle decreases and hence sheet thickness naturally increases. The limiting wall angle can be evaluated for thinning limits, depending upon the application in which the process is deployed. It can be further seen from Table 4 that as the no of forming stages increases, the spring back reduces. The spring back in the first forming stage was found to be 6.93% which followed a decreasing trend and the spring back in the top region which underwent 5 forming stages was found to be 2.81%. Similar decreasing trend was also observed in the case of FWACF fabricated by multi-stage forming strategy. So it was again established that MSRAISHF leads to better surface accuracy and more formability in the formed component.

4.4.2 Surface Finish in VWASCF. In order to further examine the effect of number of stages in RAISHF on surface quality of the formed product, the surface finish and topography of different regions of VWASCF has been studied. Samples

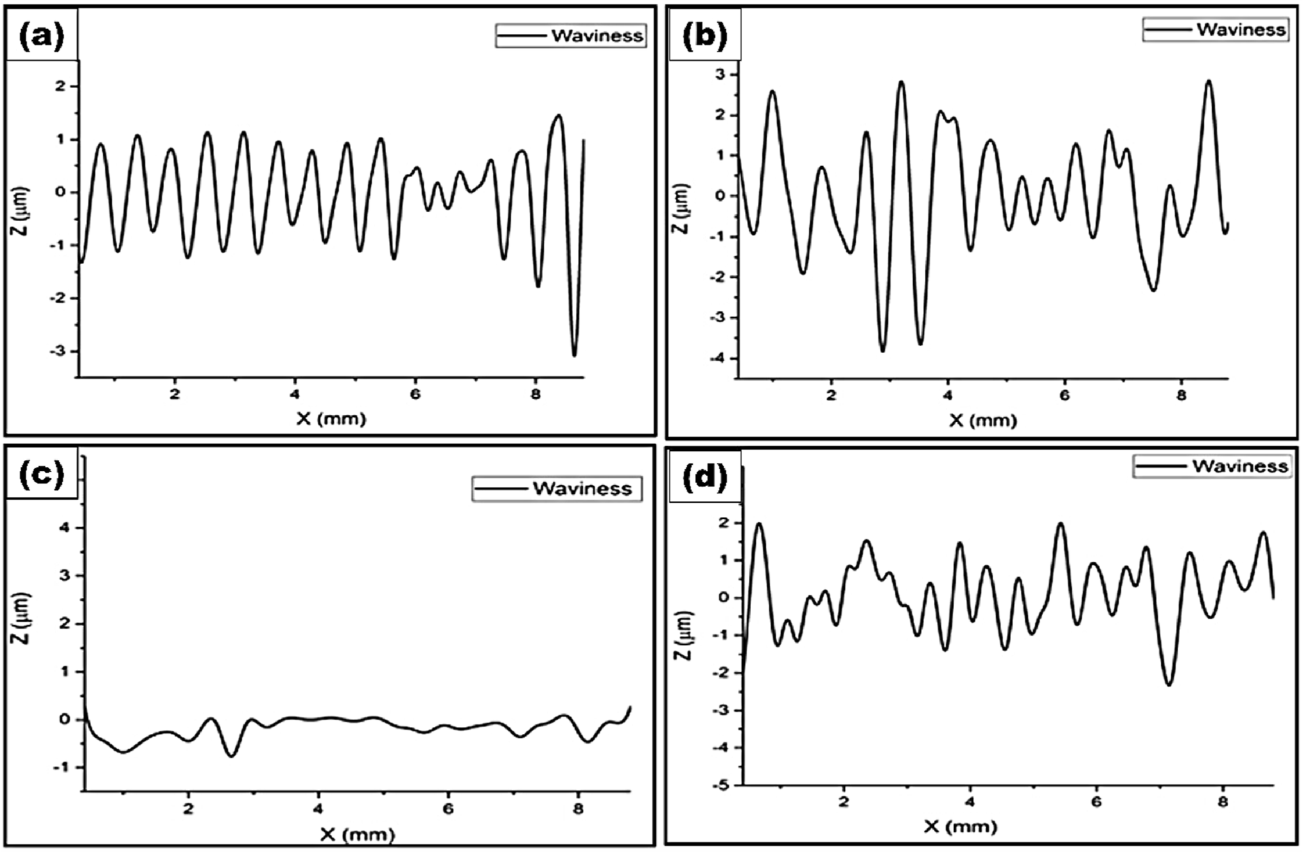

Fig. 8 Waviness plot of different surfaces: (a) inner surface of SS, (b) outer surface of SS (c) inner surface of MS (d) outer surface of MS

Table 4 Details of FWACF by single and multi-stage RAISHF

	Stage 1	Stage 2	Stage 3	Stage 4	Stage 5
Tool Diameter (mm)	12.5	12.5	12.5	12.5	12.5
Step Size (Δr)	0.4	0.28	0.19	0.14	0.11
Step Size (ΔZ)	0.4	0.4	0.4	0.4	0.4
Theoretical wall angle ($^{\circ}$)	45	55	65	70	75
No of cycles run	160	140	120	80	40
Theoretical Depth (mm)	64	56	48	32	16
Actual Depth (mm)	59.16	52.97	45.41	31.06	15.56
Initial Radius (mm)	120	120	120	120	120
Final radius (mm)	54.02	78.13	96.09	107.01	115.21
Actual Wall angle ($^{\circ}$)	41.88	51.67	62.23	67.30	72.88
Elastic Spring back (%)	6.93	6.04	4.25	3.85	2.81

have been taken from regions of VWASCF with different wall angles and surface finish analysis has been carried out on the parameters as mentioned in previous section. The 2D and 3D topographs of various regions of VWASCF are shown in Fig. 11. The step marks in the region of transition from one stage to another is visible and is depicted in dotted black regions. It is quite evident from Fig. 11(a), (b), (c), (d), (e), (f), (i), and (j) that valley height decreased continuously on increasing wall angles and increasing number of forming stages. It is evident that surface became more homogeneous as the cone was formed in more number of stages in RAISHF. The graph of average roughness in terms of R_a and R_q values with number of forming stages is shown in Fig. 12. It is quite evident from Fig. 12 that both R_a and R_q values decreased with increasing number of forming stages, and hence the formed surface became more uniform with increasing number of

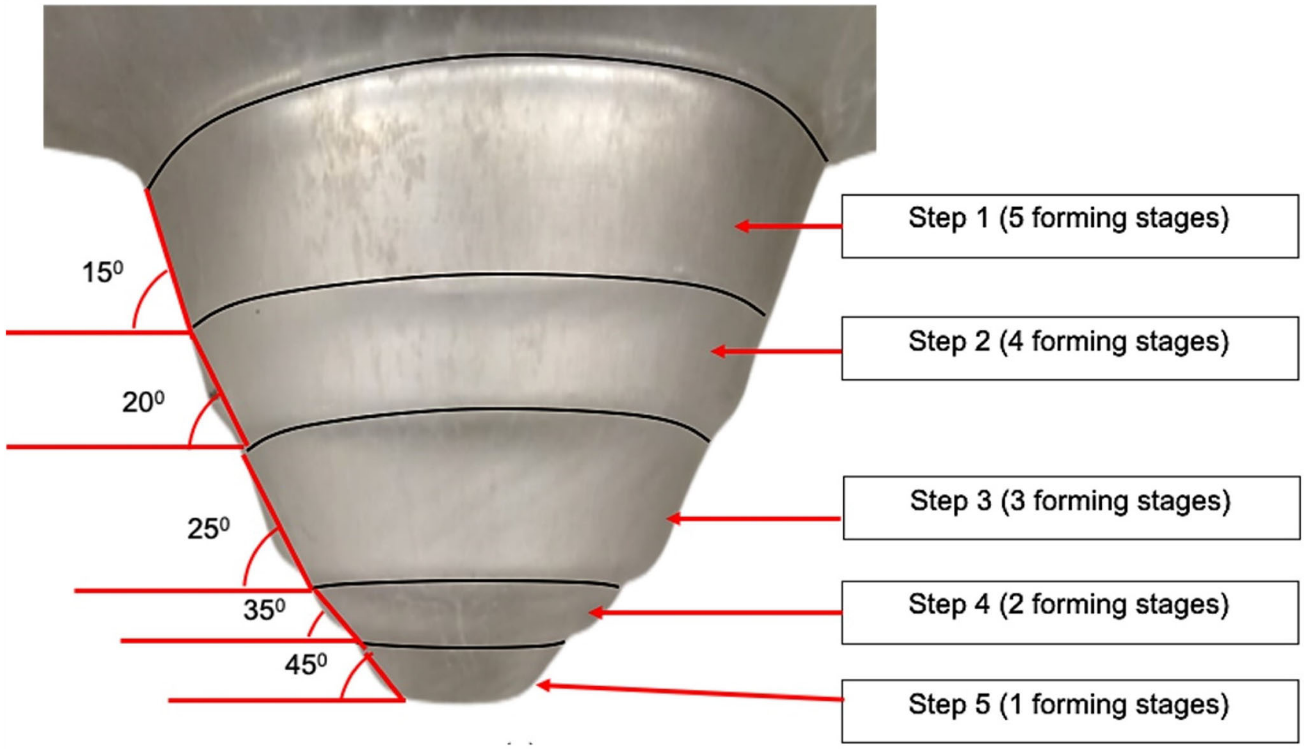

Fig. 9 Details of VWASCF made by multi-stage forming

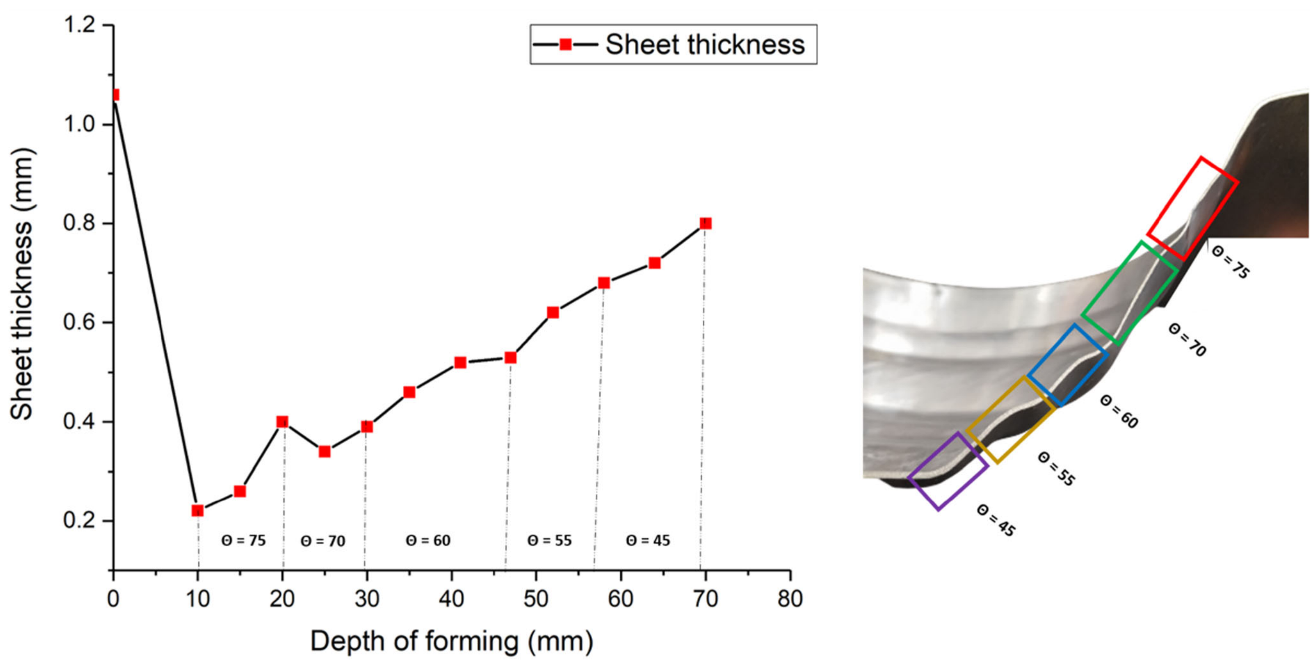

Fig. 10 Thickness distribution in regions of different wall angles in VWASCF

forming stages. After second forming stage, the R_a value decreased almost linearly from 0.534 μm to 0.32 μm as the wall angle increased from 55° after second stage, to 75° after 5^{th} stage. It can be concluded that surface finish of the product formed by multi-stage RAISHF is significantly better than that formed by single-stage RAISHF. It is recommended that the

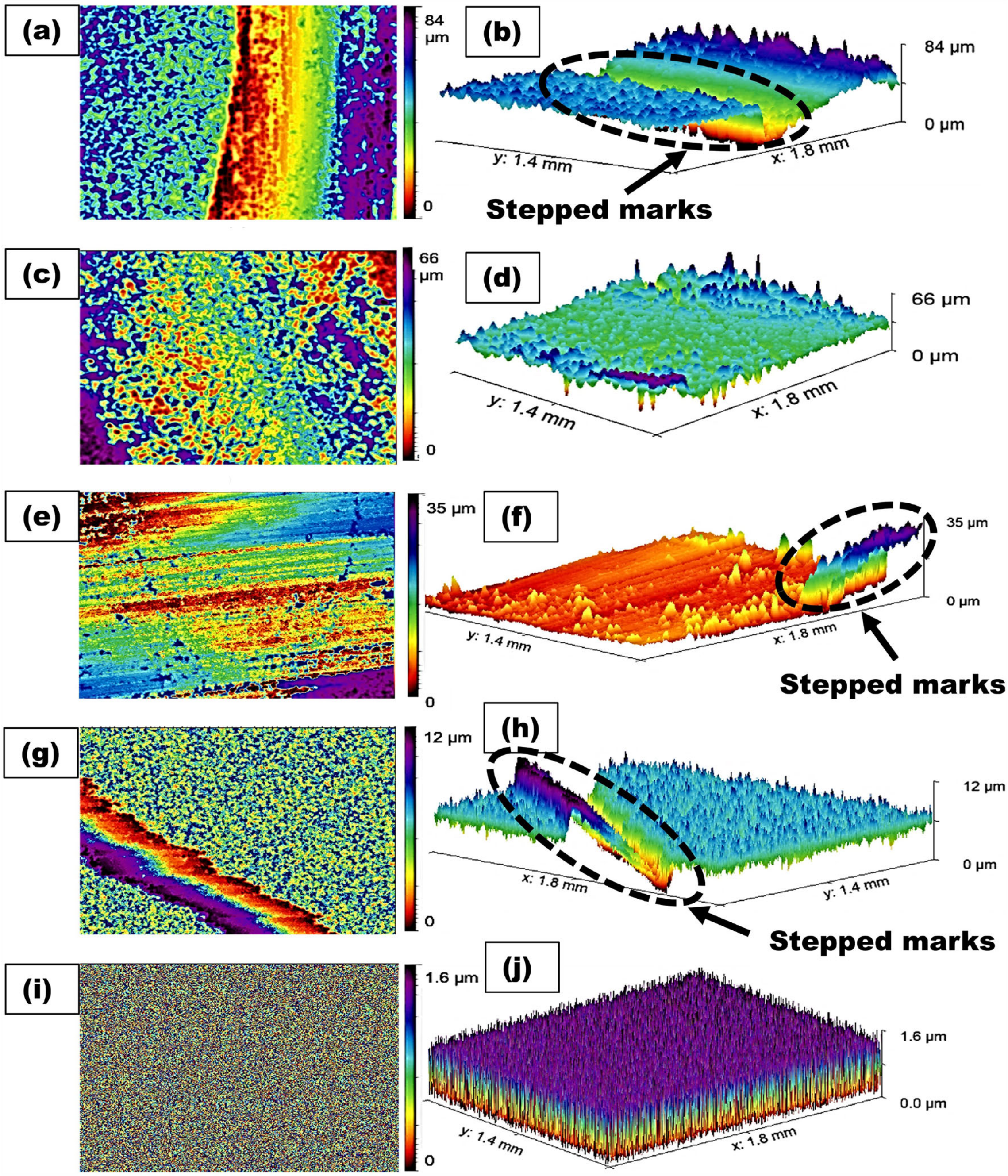

Fig. 11 Topographic micrographs of various regions of VWASCF: (a) 2D topography of 45^0 cone, (b) 3D topography of 45^0 cone, (c) 2D topography of 55^0 cone, (d) 3D topography of 55^0 cone, (e) 2D topography of 65^0 cone, (f) 3D topography of 65^0 cone, (g) 2D topography of 70^0 cone, (h) 3D topography of 70^0 cone, (i) 2D topography of 75^0 cone, (j) 3D topography of 70^0 cone

product should be formed in a double stage manner in RAISHF, as it can lead to suppression of waviness which appears in single-stage RAISHF.

5. Conclusions

In the current work, a comparison has been made between single and multi-stage RAISHF in terms of formability, thickness distribution, accuracy and surface finish of the formed product. In addition to this, a sample named VWASCF has been proposed to study the effect of the number of forming stages in multi-stage RAISHF. Following conclusions are drawn based on experiments and analysis.

- The multi-stage RAISHF process demonstrated a significant improvement in forming accuracy and depth when compared to single-stage RAISHF. The method allowed for greater forming depth at similar wall angles while minimizing spring back, ultimately enhancing the geometrical precision of the final product.
- Multi-stage RAISHF led to a more uniform thickness distribution across different regions of the formed part. The over-

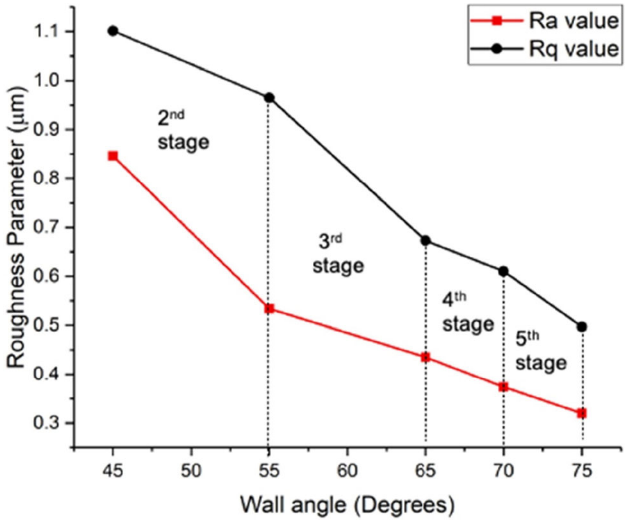

Fig. 12 Variation of R_a and R_q value in regions of different wall angles in VWASCF

all strain distribution was more uniform, especially in the middle region of the formed part, where thickness followed a consistent pattern as predicted by the sine law.

- The study found that multi-stage forming effectively reduced spring back by over 60% compared to single-stage forming. This improvement is attributed to the cumulative effect of multiple forming stages, which help stabilize the material, making it less prone to elasticity-related deformation after forming.
- The multi-stage RAISHF process significantly enhanced the surface finish of formed product compared to single-stage RAISHF. The R_a value decreased by 64.86%, from 0.925 μm to 0.325 μm, and outer surface roughness reduced from 1.751 μm to 1.192 μm. Additionally, multi-stage forming effectively minimized waviness in terms of reduced valley heights,
- A shape named VWASCF with different wall angles has been proposed to study the effect of number of forming stages in RAISHF. As the number of forming stages increased, surface quality of the cone improved and the spring back reduced significantly.

Acknowledgements

The authors are grateful to DST-SERB for sponsoring the work through project MMER/2014/0068 titled "Design, Development and Fabrication of an Incremental Sheet Hydroforming Machine Setup." E.J.B. is grateful for the UKRI Future Leaders' Fellowship funding (MR/V02261X/1) supporting this work.

Data Availability

The raw/processed data required to reproduce these findings cannot be shared at this time as the data also forms part of an ongoing study.

Conflict of interest

The authors declare that they have no conflict of interest.

Consent for publication

Consent for publication was obtained from all participants.

Open Access

References

1. J.R. Duflou, A.-M. Habraken, J. Cao, R. Malhotra, M. Bambach, D. Adams, H. Vanhove, A. Mohammadi, and J. Jeswiet, Single point incremental forming: state-of-the-art and prospects, *Int. J. Mater. Form.*, 2018, **11**, p 743–773
2. W. Emmens, G. Sebastiani, and A.H. van den Boogaard, The technology of incremental sheet forming—a brief review of the history, *J. Mater. Process. Technol.*, 2010, **210**, p 981–997
3. K. Jackson and J. Allwood, The mechanics of incremental sheet forming, *J. Mater. Process. Technol.*, 2009, **209**, p 1158–1174
4. J. Jeswiet, F. Micari, G. Hirt, A. Bramley, J. Duflou, and J. Allwood, Asymmetric single point incremental forming of sheet metal, *CIRP Ann.*, 2005, **54**, p 88–114
5. R.P. Singh, S. Kumar, P.K. Singh, M. Meraz, A.K. Srivastwa, S. Salunkhe, H. Hussein, E.S.A. Nasr, and A. Kamrani, A mathematical model for force prediction in single point incremental sheet forming with validation by experiments and simulation, *Processes*, 2023, **11**, p 1688
6. P. Gupta, A. Szekeres, and J. Jeswiet, Design and development of an aerospace component with single-point incremental forming, *Int. J. Adv. Manufact. Technol.*, 2019, **103**, p 3683–3702
7. R. Mohanraj and S. Elangovan, Incremental sheet metal forming of ti-6al-4v alloy for aerospace application, *Trans. Can. Soc. Mech. Eng.*, 2019, **44**, p 56–64
8. S. Pandre, A. Morchhale, N. Kotkunde, and S. Kurra, Processing of dp590 steel using single point incremental forming for automotive applications, *Mater. Manuf. Processes*, 2021, **36**, p 1658–1666
9. S.P. Kumar, S. Elangovan, R. Mohanraj, and S. Boopathi, Real-time applications and novel manufacturing strategies of incremental forming: An industrial perspective, *Materials Today: Proceedings*, 2021, **46**, p 8153–8164
10. M. Amino, M. Mizoguchi, Y. Terauchi, and T. Maki, Current status of "dieless" amino's incremental forming, *Procedia Engineering*, 2014, **81**, p 54–62
11. G. Kajal, M. Tyagi, and G. Kumar, A review on the effect of residual stresses in incremental sheet metal forming used in automotive and medical sectors, *Materials Today: Proceedings*, 2023, **78**, p 524–534
12. J. Wang, L. Li, P. Zhou, X. Wang, and S. Sun, Improving formability of sheet metals in incremental forming by equal diameter spiral tool path, *Int. J. Adv. Manuf. Technol.*, 2019, **101**, p 225–234
13. S. Bharti, E. Paul, A. Uthaman, H. Krishnaswamy, A. Klimchik, and R. Abraham Boby, Systematic analysis of geometric inaccuracy and its contributing factors in roboforming, *Sci. Rep.*, 2024, **14**, p 20291
14. S. Mohanty, S.P. Regalla, and Y.D. Rao, Effect of inclination and rotation of the sheet on sheet thinning and formability in robot assisted incremental sheet metal forming, *Materials Today: Proceedings*, 2021, **46**, p 1039–1049
15. R.P. Singh, S. Kumar, S. Pande, S. Salunkhe, A.E. Ragab, P.K. Singh, M. Meraz, and J.P. Davim, Robot-assisted cold and warm incremental

sheet forming of aluminum alloy 6061: a comparative study, *Metals*, 2023, **13**, p 568

16. C. Hartl, Research and advances in fundamentals and industrial applications of hydroforming, *J. Mater. Process. Technol.*, 2005, **167**, p 383–392
17. K. McLoughlin, A. Cognot, and E. Quigley, Dieless manufacturing of sheet metal components with non rigid support, *Proc. SheMet*, 2003, **2003**, p 123–130
18. J.-H. Yu, K.-S. Jung, M. Murugesan, W.-J. Chung, and C.-W. Lee, Study on the incremental sheet metal forming process using a metal foam as a die, *Int. J. Mater. Form.*, 2022, **15**, p 71
19. H. Ichihara and A. Sekiguchi, Development of elastomer-based incremental sheet forming method for curved products, *Procedia Manufacturing*, 2018, **15**, p 1184–1191
20. R.P. Singh, S.K. Gupta, P.K. Singh, and S. Kumar, Robot assisted incremental sheet forming of al6061 under static pressure: Preliminary study of thickness distribution within the deformation region, *Materials Today: Proceedings*, 2021, **47**, p 2737–2741
21. Y. Kumar and S. Kumar, Analysis of incremental sheet forming process through simulation, *Int. J. Mech. Prod. Eng. Res. Dev*, 2018, **8**, p 145–152
22. N.B. Khalifa and S. Thiery, Incremental sheet forming with active medium, *CIRP Ann.*, 2019, **68**, p 313–316
23. M. Shang, Y. Li, K. Chen, M. Yang, X. Zhao, and K. Nie, Incremental forming of hydraulic supports: a numerical and experimental study of thickness distribution, *J. Mech. Sci. Technol.*, 2023, **37**, p 6477–6491
24. M. Shang, Y. Li, M. Yang, Y. Chen, L. Bai, and P. Li, Wall thickness uniformity in isf of hydraulic support: system design, finite element analysis and experimental verification, *Machines*, 2023, **11**, p 353
25. G. Küçüktürk and H.V. Yazgın, Improvement of incremental sheet metal forming with the help of a pressurised fluid system, *Materials Testing*, 2022, **64**, p 1214–1222
26. J. Duflou, J. Verbert, B. Belkassem, J. Gu, H. Sol, C. Henrard, and A. Habraken, Process window enhancement for single point incremental forming through multi-step toolpaths, *CIRP Ann.*, 2008, **57**, p 253–256
27. R.P. Singh, S. Kumar, P.K. Singh, and M. Meraz, Experimental investigation of multi-stage robot-assisted single point incremental sheet forming of al 6061 sheet, in: Advances in Forming, Machining and Automation: Select Proceedings of AIMTDR 2021, Springer, 2022, pp. 61–69
28. Y. Kumar and S. Kumar, Experimental and analytical evaluation of incremental sheet hydro-forming strategies to produce high forming angle sheets, Heliyon 2019, 5
29. C. Raju and C.S. Narayanan, Application of a hybrid optimization technique in a multiple sheet single point incremental forming process, *Measurement*, 2016, **78**, p 296–308
30. S. Kurra and S.P. Regalla, Experimental and numerical studies on formability of extra-deep drawing steel in incremental sheet metal forming, *J. Market. Res.*, 2014, **3**, p 158–171
31. R. Crina, Determination of the maximum forming angle of some carbon steel metal sheets, *J. Eng. Stud. Res.*, 2011, **17**, p 71
32. L.R. Zhou, The effect of forming half-apex angle on incremental sheet metal forming, *Adv. Mater. Res.*, 2010, **139**, p 1514–1517
33. A. Habraken, Single point incremental forming to increase material knowledge and production flexibility, in: Journal of Physics: Conference Series, volume 734, IOP Publishing, 2016, p. 032130
34. M. Silva and P. Martins, Two-point incremental forming with partial die: theory and experimentation, *J. Mater. Eng. Perform.*, 2013, **22**, p 1018–1027
35. Z. Liu, W.J. Daniel, Y. Li, S. Liu, and P.A. Meehan, Multi-pass deformation design for incremental sheet forming: analytical modeling, finite element analysis and experimental validation, *J. Mater. Process. Technol.*, 2014, **214**, p 620–634
36. M. Shamsari, M.J. Mirnia, M. Elyasi, and H. Baseri, Formability improvement in single point incremental forming of truncated cone using a two-stage hybrid deformation strategy, *Int. J. Adv. Manuf. Technol.*, 2018, **94**, p 2357–2368
37. E. Ndip-Agbor, P. Cheng, N. Moser, K. Ehmann, and J. Cao, Prediction of rigid body motion in multi-pass single point incremental forming, *J. Mater. Process. Technol.*, 2019, **269**, p 117–127
38. J. Verbert, B. Belkassem, C. Henrard, A. Habraken, J. Gu, H. Sol, B. Lauwers, and J. Duflou, Multi-step toolpath approach to overcome forming limitations in single point incremental forming, *Int. J. Mater. Form.*, 2008, **1**, p 1203–1206
39. R. Malhotra, A. Bhattacharya, A. Kumar, N. Reddy, and J. Cao, A new methodology for multi-pass single point incremental forming with mixed toolpaths, *CIRP Ann.*, 2011, **60**, p 323–326
40. P. Dai, Z. Chang, M. Li, and J. Chen, Reduction of geometric deviation by multi-pass incremental forming combined with tool path compensation for non-axisymmetric aluminum alloy component with stepped feature, *Int. J. Adv. Manuf. Technol.*, 2019, **102**, p 809–817
41. H.K. Nirala, P.K. Jain, J. Roy, M. Samal, and P. Tandon, An approach to eliminate stepped features in multistage incremental sheet forming process: Experimental and fea analysis, *J. Mech. Sci. Technol.*, 2017, **31**, p 599–604
42. S. Thiery and N. Ben Khalifa, Geometrical accuracy in two-stage incremental sheet forming with active medium, in: Production at the Leading Edge of Technology: Proceedings of the 11th Congress of the German Academic Association for Production Technology (WGP), Dresden, September 2021, Springer, 2022, pp. 65–74
43. A.H. Naronikar, H.A. Jamadagni, A. Simha, and B. Saikiran, Optimizing the heat treatment parameters of al-6061 required for better formability, *Materials Today: Proceedings*, 2018, **5**, p 24240–24247
44. ASTM E8/E8M-15a, Standard Test Methods for Tension Testing of Metallic Materials, ASTM International, West Conshohocken, PA, 2015. https://www.astm.org
45. ASTM E643-15, Standard Test Method for Ball Punch Deformation of Metallic Sheet Material, ASTM International, West Conshohocken, PA, 2015
46. S. Kumar and Y. Kumar, Robot assisted high speed incremental sheet hydroforming machine
47. R.P. Singh, S. Kumar, P.K. Singh, M. Meraz, S. Salunkhe, Advancements in robot-assisted incremental sheet hydroforming: a comparative analysis of formability, mechanical properties, and surface finish for rhomboidal and conical frustums, International Journal of Intelligent Robotics and Applications 2024, 1–13
48. R.P. Singh, S. Kumar, E.J. Brambley, S. Choudhary, P.K. Singh, and S. Dhara, Optimizing formability of incremental sheet forming using the straight groove test assessed with a variable wall angle conical frustum, *Manufacturing Letters*, 2025, **44**, p 453–465
49. G. Hussain, N. Hayat, and G. Lin, Pyramid as test geometry to evaluate formability in incremental forming: Recent results, *J. Mech. Sci. Technol.*, 2012, **26**, p 2337–2345
50. G. Ambrogio, L. Filice, F. Gagliardi, and F. Micari, Sheet thinning prediction in single point incremental forming, *Adv. Mater. Res.*, 2005, **6**, p 479–486
51. J.H. Kim, J.H. Park, and C. Kim, A study on the mechanics of shear spinning of cones, *J. Mech. Sci. Technol.*, 2006, **20**, p 806–818
52. B. Avitzur and C. Yang, Analysis of power spinning of cones 1960
53. X. Li, K. Han, Z. Li, D. Li, and L. Zhang, One novel method to improve surface quality in incremental sheet forming, *Procedia Eng.*, 2017, **207**, p 842–847
54. M. Ortiz, M. Penalva, E. Iriondo, and L.N. López de Lacalle, Accuracy and surface quality improvements in the manufacturing of ti-6al-4v parts using hot single point incremental forming, *Metals*, 2019, **9**, p 697
55. E. Hagan and J. Jeswiet, Analysis of surface roughness for parts formed by computer numerical controlled incremental forming, *Proc. Inst. Mech. Eng., Part B: J. Eng. Manuf.*, 2004, **218**, p 1307–1312
56. M. Silva, M. Skjødt, P.A. Martins, and N. Bay, Revisiting the fundamentals of single point incremental forming by means of membrane analysis, *Int. J. Mach. Tools Manuf*, 2008, **48**, p 73–83

Publisher's Note Springer Nature remains neutral with regard to jurisdictional claims in published maps and institutional affiliations.